Title

An Agent-Based Model of School Closing in Under-Vacccinated Communities During Measles Outbreaks.

Journal

Agent-Directed Simulation Symposium (ADS). Agent-directed Simulation Symposium, 2016(5)

ISSN

0037-5497

Authors

Getz, Wayne M
Carlson, Colin
Dougherty, Eric
et al.

Publication Date

2016-04-01

DOI

10.1177/0037549717721754

Peer reviewed

Special Issue

Simulation

Simulation: Transactions of the Society for Modeling and Simulation International
1–9

DOI: 10.1177/0037549717721754
journals.sagepub.com/home/sim
SAGE SCS

An agent-based model of school closing in under-vaccinated communities during measles outbreaks

Wayne M Getz[1,2], Colin Carlson[1], Eric Dougherty[1], Travis C Porco[3] and Richard Salter[4]

Abstract

The winter 2014–15 measles outbreak in the United States represents a significant crisis in the emergence of a functionally extirpated pathogen. Conclusively linking this outbreak to decreases in the measles, mumps, and rubella (MMR) vaccination rate (driven by anti-vaccine sentiment) is critical to motivating MMR vaccination. We used the NOVA modeling platform to build a stochastic, spatially-structured, individual-based SEIR model of outbreaks, under the assumption that $R_0 \approx 7$ for measles. We show this implies that herd immunity requires vaccination coverage of greater than approximately 85%. We used a network structured version of our NOVA model that involved two communities, one at the relatively low coverage of 85% coverage and one at the higher coverage of 95%, both of which had 400-student schools embedded, as well as students occasionally visiting superspreading sites (e.g., high-density theme parks, and cinemas). These two vaccination coverage levels are within the range of values occurring across Californian counties. Transmission rates at schools and superspreading sites were arbitrarily set to respectively 5 and 15 times the background community rates. Simulations of our model demonstrate that a 'send unvaccinated students home' policy in low coverage counties is extremely effective at shutting down outbreaks of measles.

Keywords

Superspreaders, epidemiological models, NOVA software platform, herd immunity, R-zero.

1 Introduction

A recent reemergence of measles in the United States (US) provides us with an opportunity to think more deeply about vaccinations in modern societies and their role in providing protection against viral diseases. Measles is caused by a Morbillivirus (family: Paramyxoviridea) that is expelled from an infected individual during coughing or sneezing. The virus can remain infectious for several hours in the form of aerosolized droplets or fomite residues.[1] As a consequence of near life-long immunity in individuals that have recovered from the disease, prior to large-scale vaccination programs in Europe and the US, measles outbreaks were seasonally linked to new cohorts of young children entering school for the first time.[2] The endemicity of this process in developed-world cities with relatively large populations (at least 250,000–500,000 individuals) has been explained with the aid of mathematically sophisticated models.[3] Such seasonal outbreak patterns were eliminated in the US after 1981, through the implementation of the highly effective MMR (measles, mumps, and rubella) blanket vaccination program.[4]

The principle of vaccinating a population beyond its 'herd immunity' threshold lies at the heart of the continued success of the US MMR vaccination program.[5,6] The threshold ratio of vaccinated to unvaccinated individuals for a herd-immune population—that is, a population where this ratio is sufficiently high to cause infections to rapidly fade out rather than break out—depends upon the basic reproductive number, R_0 (the expected number of cases caused by the index case when the whole population is susceptible) for the disease. The value of R_0 itself is influenced by the infectiousness of the pathogen, the lengths of time that infected individuals are infectious, and contact

[1]Department ESPM, UC Berkeley, CA, USA
[2]School of Mathematical Sciences, UKZN, Republic of South Africa
[3]Francis I Proctor Foundation, Department of Epidemiology & Biostatistics, UC San Francisco, CA, USA
[4]Department of Computer Sciences, Oberlin, OH, USA

Corresponding author:
Wayne M Getz, Department ESPM, UC Berkeley, 130 Mulford Hall, Berkeley, CA 94720, USA.
Email: wgetz@berkeley.edu

rates among individuals within the community. Thus, in essence, the efficacy of a vaccination program depends on both complex immunological and sociological processes that can be analyzed in the context of dynamic game theory.[7]

The immunological process component involves optimal ages and dosages at which to administer vaccines of various kinds (e.g., attenuated live vaccine, as in MMR, or inactivated virus, as in Polio iPV), or segments of virus (influenza injections), one dose, or primary dose plus boosters, and so on. MMR vaccinations may fail if the primary dose is given to infants protected by maternal antibodies transferred during breastfeeding.[8] Avidity testing can be used to assess the efficacy of vaccinations, but such tests are not widely utilized in measles epidemiology.[9] Thus, it can be misleading to take statistical data at face value regarding assumed levels of protection for given levels of a vaccination coverage.[10]

The sociological process component enables misinformation to shape outbreak dynamics. For example, influenced by a now retracted study in *The Lancet* in 1998 that linked the MMR vaccine to autism,[11] a significant minority of parents, clustered in particular geographic regions around the US, refused MMR vaccinations for their children.[12] Even after the retraction of the study, these groups persist, and despite major efforts to remediate the damage, recent results confirm that these self-proclaimed 'anti-vaxxers' respond negatively to educational campaigns, becoming more staunchly opposed to vaccination.[13] As a consequence of anti-vaxxer groups, including those opposed for religious purposes (e.g., the Amish in Ohio), measles outbreaks are now more likely in the US: the US Center for Disease Control reported 911 cases for the decade 2001–2011[14] (which is fewer than 8 cases per month), while close to 650 cases were reported in 2014, dominated by an outbreak in the Amish community in Ohio, and more than 100 for the month of January in 2015, dominated by cases in California linked to the so-called Disneyland outbreak.[15,16] Thus, the sociological component includes a growing 'small world' phenomenon, with individuals making contact at high-density entertainment venues that increasingly draw in patrons from considerable distances, and then serve as superspreading centers for highly contagious respiratory diseases, such as measles. 'Superspreading', defined as a process whereby a few individuals cause a disproportionately large number of secondary infections, has been considered in terms of individual and environmental heterogeneity.[17] Individuals with high pathogen shedding rates[18] or longer periods of infectiousness[19] may lead to greater numbers of secondary infections. Similarly, superspreading centers can be viewed as discrete environmental patches that provide opportunities for significantly higher contact rates than predicted by expected movement patterns.[20]

Spatial heterogeneity in the effective vaccination rates alters the likelihood with which outbreaks occur. While herd immunity levels may exist at some of the originating sites of individuals visiting a superspreading center, unvaccinated individuals from those sites may carry the disease back to keep feeding a continuous low-level stream of cases at sites with vaccination rate above herd immunity levels, as well as starting self-sustaining outbreaks at sites with vaccination rates below levels of herd immunity. Here we evaluate the efficacy of 'stay-at-home regulations' for children who are not vaccinated in schools were outbreaks occur.

2 Model

2.1 Motivation for approach

The prevailing paradigm for modeling epidemics is to use systems of deterministic or stochastic differential or difference equations that divide the population into disease (e.g., susceptible, infected, recovered, immune) classes,[21] as well as other demographic (e.g., age, sex) and behavioral classes (e.g., sexually active) and to fit transmission, recovery, and other relevant parameters using least-squares estimation (LSE)[22] or maximum likelihood estimation methods,[23] based on comparisons of model output and empirical data. Going back to the work of Frost and Reed,[24] a second approach to modeling epidemics has been to follow transmission chains (incidence and offspring distributions, transmission trees and branches), generally considered within the framework of semi-Markov branching process.[24] While the first paradigm is most useful for large-scale epidemics involving infection of a significant fraction of the susceptible population (i.e., $> 1\%$), which is the case inter alia for influenza—HIV, tuberculosis, and measles in unvaccinated communities; the second is most useful for emerging diseases when the proportion infected is often very small (i.e., $< 0.1\%$)—which includes inter alia, severe acute respiratory syndrome (SARS),[25] Ebola,[26] and hantavirus, as well as measles in communities where vaccination rates are close to herd immunity threshold levels.[27,16]

Given our interest in disease outbreak dynamics, the analysis we report here is based on a Markov chain approach, as discussed by Chowell et al.[21] but modified to allow for the implications and efficacy of key interventions that need to be evaluated. Our model of a measles outbreak in the US explicitly includes barring unvaccinated school-aged individuals from attending schools when one or more individuals in the school have come down with the measles because of its viability as an affective outbreak mitigation strategy.[28] It also allows for a reduction in transmission rates over the course of the epidemics due to behavioral changes that reduce contact rates in the community between sick and uninfected individuals,

as the community becomes more informed on how to interact with infectious individuals.[29] Our model is unique in dividing the population at risk during a measles epidemic into school and general population components with a metapopulation structure that includes vaccination levels both above and below the herd immunity level.

2.2 Transmission chain formulation

Most epidemiological models begin by dividing the population into 'susceptible' (S) and 'infected + infectious' (I) individuals, while elaborations discriminate between 'exposed but not yet infectious' (E) and 'infectious' (I), as well as 'removed' (R),[30] where the latter can be broken down into 'dead' (D) and 'recovered with some level of acquired immunity' (V).[31] Although some measles models have treated the epidemic as an SIR process,[32] many others have included an E class.[33] We include the latter because in measles the period that an individual is infected but not yet infectious is of similar length to the infectious period itself (in fact it can be more than twice as long—cf. Table 3 in Cauchemez and Ferguson[34]), and this can have a destabilizing impact on the dynamics of epidemiological process.[35] We emphasized here that we need not specify the size of the S-class involved, but rather assume some level of 'risk-of-infection' that is proportional to the number of infected individuals in the subpopulation of interest, where subpopulations form an interconnected metapopulation, and 'risks-of-infection are subpopulation dependent. Thus we model the disease incidence rate in time period $[t, t+1]$ (t in our case will represent days) in subpopulation j containing $I_j(t)$ infectious individuals, using Monte Carlo methods, from a Poisson distributions with mean as follows:

$$m_j(t) = \lambda_j I(t) \tag{1}$$

to generate $E_i(t+1)$. (Note: Roman font S, I, and E name the class, while italic font $I_j(t)$ and $E_j(t)$ refer to the number of individuals at time t in so-named class of subpopulation j).

Ignoring the population designation index j for the moment, the more usual approach to characterizing transmission is to assume that, for some 'transmission intensity constant' $\beta > 0$, the incidence rate is determined by the expression $m(t) = \beta S(t) I(t)$ in the case of density-dependent transmission and by $m(t) = \beta S(t) I(t)/N(t)$ in the case of frequency-dependent transmission.[31,36,37] This approach has been generalized to assume that, for some population scaling constant $K > 0$, transmission is more generally characterized by the following function, which includes both density-dependent ($K \to \infty$) and frequency-dependent ($K \to 0$ with appropriate rescaling of β) transmission as limiting cases:

$$m(t) = \beta S(t) \frac{I(t)}{1 + N(t)/K} \tag{2}$$

This latter characterization requires that both S and N are known when, by analogy (i.e., comparison of Equation (3) and (2), with index j ignored), the values of S and N are used to determine the value as follows:

$$\lambda(S, N) = \frac{\beta S}{1 + N/K} \tag{3}$$

An alternative approach is to use the fact that when outbreaks occur $I \ll S$, or equivalently, $S \approx N$, so that $\lambda \approx \frac{\beta}{1/N + 1/K}$, or when $N \gg K$, $\lambda \approx K\beta$. Thus, in relatively large populations, the incidence rate becomes density-independent and can be modeled by a stochastic Poisson process, following the approach we take below.

The model focuses on individuals in the population that become exposed to an individual in state I at time t, and follows their progress over time as they make transitions from states E to I to R (most of which are now in state V—i.e., immune, but a small percent transition to D—i.e., death). In a totally naïve population, each individual in state I at time t generates on average λ individuals in state E at time $t+1$, using Poisson statistics. In a population in which a proportion p_v are vaccinated, this expected number is modified by the value $(1 - p_v)$: specifically, if the Poisson drawing yields r individuals to be assigned the state E, then each of these individuals is moved to state V with probability p_v. Thus, in short, the incidence rate at time $t+1$ will follow a Poisson distribution with expected value $(1 - p_v)\lambda I(t)$. If we use the time variable s to denote individuals at time t that became infected with the disease at time $(t - s)$, then letting $U(t, s)$ represents the number of exposed individuals at time t who were exposed s days ago, it follows that the dependent variable $U(t, 0)$ is the incidence at time t: i.e., as follows:

$$U(t+1, 0) = (1 - p_v)\lambda I(t) \tag{4}$$

For the sake of simplicity, assume the latent period $[0, s_1]$ is the same for all individuals. Similarly, assume all individuals have the same infectious period $[s_1, s_1 + s_2 - 1]$. Thus, for all individuals exposed to the pathogen at any time $t = 1, 2, \ldots$, $s_1 > 0$ and $s_2 > 0$ are constants rather than random variables across individuals. It then follows that these individuals are infected (exposed) but not yet infectious for the first $s_1 - 1$ periods of time, becoming infectious s_1 units after first exposure, and that they remain infectious for $s_2 - 1$ periods of time. Thus, all individuals make the transition to R status $s_1 + s_2$ periods of time after first exposure. Under these assumptions of constant latent and infectious periods, and assuming that individuals enter the R state only after s_2 units of time, it follows that:

$$I(t) = \sum_{k=1}^{s_2} U(t, s_1 + k - 1) \quad (5)$$

The most efficient implementation of a homogeneous version of the model is to aggregate individuals by states as follows:

$$Q_i(t) \equiv U(t, i-1),\ i = 1, ..., s_1 + s_2$$

(i.e., time units since the exposure/transmission), and model how numbers in each state change over time using the following equations (where the notation $x \sim \text{POISSON}[m]$ implies a random drawing from a Poisson distribution with parameter m) as follows:

$$\begin{aligned} Q_1(t+1) &\sim \text{POISSON}[(1-p_v)\lambda \sum_{k=1}^{s_2} Q_{k+s_1-1}(t)] \\ Q_i(t+1) &= Q_{i-1}(t) \quad i = 2, ..., s_1 + s_2 \end{aligned} \quad (6)$$

2.3 Individual-based NOVA model

A less efficient, but more comprehensive implementation that allows us to keep track of individuals as they may move through space or exhibit variation in susceptibility, length of latent period (i.e., variation in s_1 among individuals), length of infection (variation in s_2), and risk of mortality while ill (not included in the above model), all possibly as functions of genetic or individual level environmental factors, is to follow the progress of each individual recruited to the population using Equation (4) to link individuals to parents, rather than Equation (5) (which only counts incidence at an aggregated group level). Here we took this individual-based approach, because we wanted to keep track of the 'next-generation distribution' to obtain estimates of R_0 from this distribution, with the details of how to do this described elsewhere.[19,26] We also wanted to follow individuals as they are influenced by spatial factors: in our case children in the local community environments with different vaccination coverage rates and including time spent at schools where transmission rates are higher. The constant values we used for the latent and infectious period designators were $s_1 = 7$ and $s_2 = 3$ days, based on data listed elsewhere (cf. Table 3 in Cauchemez and Ferguson[34]), with the assumption of constancy due to the fact that the natural variability in these numbers across individuals is not well characterized in specific communities. There are many reasons why s_2, in particular, is not well known, including the fact that in different communities, detection of disease and implementation of treatment vary greatly. Thus, the true infectious period is considerably longer than $s_2 = 3$ days, but the value we use represent an estimate of the 'effective' number of days during which individuals are available to transmit to other members of their local community prior to isolation and treatment. Aside from this, estimates of the incidence rate parameter λ will, to a large extent, vary collinearly with values of s_1 and s_2.

2.4 Spatial structure and incidence rates

Many different factors affect transmission and hence incidence rates: changes in the virulence of strains over time,[38] the movement behavior of individuals within populations, the size of those populations, disease detection and treatment protocols that influence how early symptoms are recognized, and how strict patient isolation practices are. It is therefore unsurprising that estimates of R_0 for highly contagious diseases such as measles can vary by several hundred percent. We based our selection for the parameter λ introduced in Equation (1) on our expectation that in an unvaccinated population the value of R_0 should be somewhere in the range $[6.2, 7.7]$.[10] Following a heuristic procedure of trying out different values of λ, with $s_1 = 7$ and $s_2 = 3$, we found that $\lambda = 2.2$ yielded a value of $R_0 = 6.6$ for the case $p_v = 0$. Further, we ran the model 10 times for each of the values of $p_v = 0.05,\ 0.1,\ \ldots, 0.75, 0.80$, to obtain estimates of $R_0(p_v)$ from the next-generation distribution that our simulations produced after running the model for 40 days after the introduction of a single index case (i.e., patient zero) into the population.

The results of these estimates are plotted in Figure 1. In this figure, we see that the regression line through the simulation data intersects the point $(p_v, R_0) = (1, 0)$ as expected (i.e., the absence of susceptible individuals necessarily implies $R_0 = 0$). This regression line also indicates that $p_v = 0.85$ is the herd immunity threshold vaccination level, because $R_0(0.85) = 1$. This estimate could have been made directly by drawing a line from the point $(1, 0)$ to $(0, 6.6)$ and calculating the point on this line that would

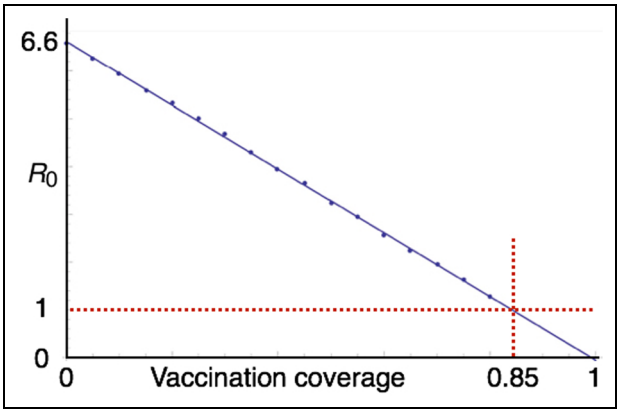

Figure 1. A regression line through estimates of R_0 obtained via simulation for populations with different levels of vaccination coverage (p_v). Note that $p_v = 0.85$ corresponds to $R_0 = 1$, implying that a vaccination rate of 85% coverage is needed to achieve the herd immunity threshold.

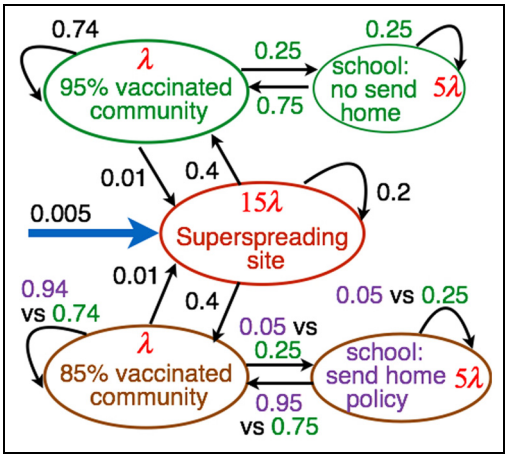

Figure 2. A graphical image of Table 1 from the 2013–2014 Kindergarten Immunization Assessment Results, California Department of Public Health (CDPH), Immunization Branch, available from CDPH (download pdf).
MMR: measles, mumps, rubella

yield $R_0 = 1$ or, equivalently, using the following well-known formula for critical coverage in a homogenous, well-mixed population: $1 - 1/R_0 = 1 - 1/6.6 = 0.85$. The data generated from our simulations, however, show that 10 runs are sufficient to provide an excellent estimate of the value for each of the points plotted in Figure 1.

Following the above procedure for estimating a suitable value for λ, once s_1 and s_2 had been selected from reports in the literature, and a target value of R_0 identified, we designed a spatial configuration that could be used to test the efficacy of a 'send unvaccinated students home' policy for schools to control outbreaks in situations where the vaccination coverage in the school is relatively low. In particular, we set up two communities, one vaccinated around the herd immunity threshold level (low coverage: 85%) and one vaccinated well above the herd immunity threshold level (high coverage: 95%). For purposes of comparison, we refer to the data provided in Figure 2. These data reflect a 92.3% for the recommended two doses of MMR. True protection is likely somewhat higher because of individual who have received a one-dose vaccination. The values specified in Figure 3, when infected individuals in under-vaccinated communities are not sent home, correspond to the transition matrix (order of variables, following Figure 3, is 'superspreading sites', '95% community', 'school in 95% community', '85% community', 'school in 85% community 2') as follows:

$$T_0 = \begin{pmatrix} 0.2 & 0.01 & 0 & 0.01 & 0 \\ 0.4 & 0.74 & 0.75 & 0 & 0 \\ 0 & 0.25 & 0.25 & 0 & 0 \\ 0.4 & 0 & 0 & 0.74 & 0.75 \\ 0 & 0 & 0 & 0.25 & 0.25 \end{pmatrix}$$

and when individuals are sent home to the matrix as follows:

	All	Public	Private
Number of Schools	7684	5852	1832
Number of Students	533,680	491,905	41,775
All Required Immunizations	90.2%	90.6%	85.4%
Conditional Entrants	6.5%	6.3%	8.5%
Permanent Medical Exemptions	0.19%	0.18%	0.29%
Personal Belief Exemptions	3.15%	2.92%	5.88%
4+ DTP	92.2%	92.5%	88.6%
3+ Polio	92.6%	93.0%	88.5%
2+ MMR	92.3%	92.7%	87.6%
3+ Hep B	94.8%	95.0%	91.8%
1+ Vari (or physician-documented disease)	95.3%	95.5%	92.1%

Figure 3. The spatial structure of our stochastic model depicting probabilities of daily movements of individuals between home community and school as well as visits to superspreading sites, such as entertainment centers. The black and green transition rates correspond to the stochastic matrix T_0 provided in the text. When the purple values are substituted for the green values in the under-vaccinated community (i.e., 85% vaccination coverage) we obtain a 'send home policy' effect, modeled by stochastic matrix T_h. The implications of these transition rates for time spent at different sites are discussed in the text. The solid blue input vector represents a small probability that during the course of an outbreak infected individuals may be imported into the system from an origin other than the two explicitly modeled communities. The incidence rate parameter values, indicated in red, are $\lambda = 2.2$ within the community, but 5 times this rate within schools and 15 times this rate at the superspreading site.
vs: versus

$$T_h = \begin{pmatrix} 0.2 & 0.01 & 0 & 0.01 & 0 \\ 0.4 & 0.74 & 0.75 & 0 & 0 \\ 0 & 0.25 & 0.25 & 0 & 0 \\ 0.4 & 0 & 0 & 0.94 & 0.95 \\ 0 & 0 & 0 & 0.25 & 0.05 \end{pmatrix}$$

The dominant eigenvectors that characterize the stable probability distributions associated with stochastic matrices T_0 and T_h respectively (i.e., the eigenvectors corresponding the eigenvalue that has value 1) are $(0.009, 0.3715, 0.124, 0.3715, 0.124)'$ and $(0.010, 0.415, 0.138, 0.415, 0.022)'$.

2.5 Accessing the model

As mentioned above, the model was built using the NOVA modeling platform, which is downloadable for free at the Novamodeler website.[39,26,40] The NOVA file for the model is available at the Getz Lab Website (NOVA models download: Measles, Spring Simulation Conference, 2016). A web-based implementation of the model can be accessed at the NOVA OnLine Model Library (username and password are both 'numerus').

3 Results

The first study we undertook was to identify a value for the transmission parameter λ and then to characterize how the disease outbreak threshold, as represented by $R_0(p_v)$, varied with vaccination coverage parameter $p_v \in [0, 1]$. We settled on the value $\lambda = 2.2$, which we confirm corresponds to $R_0(0) = 6.6$ (unvaccinated population) and $R_0(0.85) = 1$ (herd immunity threshold for vaccination coverage), as illustrated in Figure 1.

We then used our simulation model to compare outbreak sizes in a five compartment system that has the structure depicted in Figure 3: viz., two communities, one with 85% vaccination coverage the other with 95% vaccination coverage, both containing schools where students experience a disease transmission hazard that is 5 times the background community rate and both sending individuals to superspreading sites (represented by a single spatial compartment, but may in fact be a collection of sites) for limited periods of time where the disease transmission hazard is 15 times that of the background community and, hence, 3 times that at schools. We note, however, that in the school environment we took account of the fact that the population size is relatively small compared with the community at large. So in the school environment we reduced the risk of transmission by a factor $(S_{\text{school}}/N_{\text{school}}(t)$, where we set $N_{\text{school}} = 400$ and $S_{\text{school}}(t)$ is the number of individuals at that school that remained susceptible in not yet being infected or sent home by time t). From the dominant eigenvector associated with the matrices T_0 we confirm that under a 'no action' policy infectious individuals in both communities spend approximately 74% of their time in the local community/home environment (incidence rate is given by λ), 25% at school (incidence rate 5λ), and 1% at superspreading centers/sites (incidence rate 15λ). Similarly, from the dominant eigenvector associated with the matrix T_h it follows that under a 'send unvaccinated students home' policy, during the course of an outbreak, infectious individuals in the first community spend their time, as specified for T_0 while, individuals in the second community now spend approximately 94% of their time at in the local community/home environment, only 5% at school, and again approximately 1% of their time at superspreading centers/sites.

Table 1. Comparison of number of cases under 'no action' versus 'send unvaccinated students home' policy.

Communities	No action	Send home
85% vaccination coverage	348 ± 403	2.4 ± 3.5
95% vaccination coverage	42 ± 50	1.6 ± 1.5
To superspreader site	4.9 ± 6.1	0.2 ± 0.6

We run our spatial model 100 times for each of the two cases: 'no action' and a 'send unvaccinated students home' policy. In each case, each run terminated either with the fading of the outbreak (no infectious cases possible) or after 200 days, which ever came first. The average and standard deviation of the results obtained from each set of 100 runs are reported in Table 1; density plots of resulting distributions of case number are illustrated in Figure 4.

4 Discussion

When modeling highly heterogeneous and stochastic processes, while endeavoring to maintain generalizability beyond the particular set of circumstances under consideration, a number of simplifying assumptions must be made. At each step in this process, uncertainty inevitably increases. Hence model validation is particularly difficult because being stochastic, any outbreak we observed is but one manifestation of a distribution of possible trajectories that can vary from fadeout to dramatic outbreak for an epidemic governed by the identical set of process parameter values (cf. results presented by Lloyd[26] in the context of the recent Ebola outbreak in West Africa). Thus, we focus here on results from an analysis that allows us to evaluate the efficacy of 'send home' policies as a way of extinguishing an outbreak of a highly transmissible disease, such as measles. We can do this without knowing the precise values of actual epidemiological process parameters, if we are in the right ball park with regard to the general character of the epidemic, because it is the comparative results from fully-vaccinated versus under-vaccinated

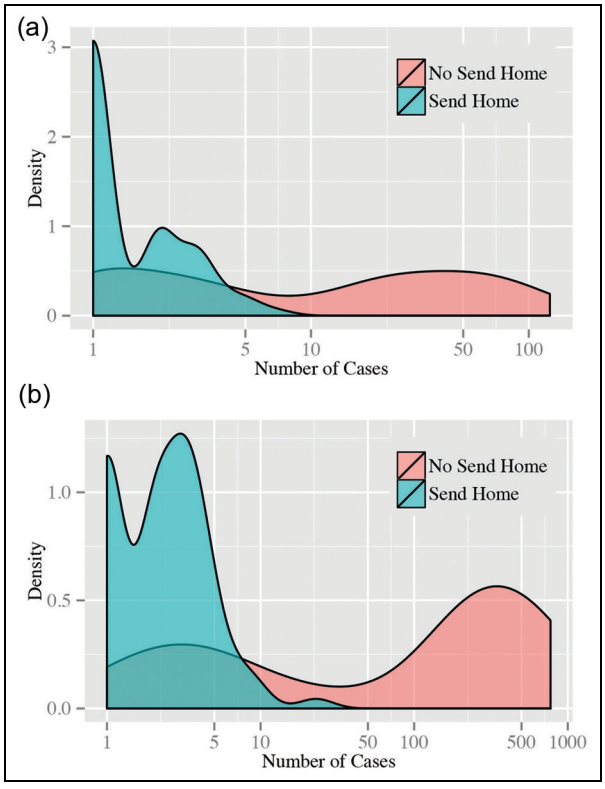

Figure 4. Probability density plots of log number of cases from 100 runs of the model for each of the with and without implementation of the 'send unvaccinated students home' policy cases: (a) low vaccination rate community (85%); (b) high vaccination rate community (95%) (note: the abscissa scale is different from case (a).

communities that is critical. We know that we are in the right ball park because our model is based on R_0 values, transmission rates, various contact rates, and infectiousness period durations obtained from the literature,[10] as well as vaccination rates obtained from the California Department of Health. In addition, we stress that there, each measles outbreak appears to follow its own unique set of parameter values, as societal structures evolve and population levels of susceptibility change with ever changing vaccination policies. Nonetheless, the strength of the methods presented here lie in their ability to be easily adjusted based on information gathered from current outbreaks. Thus, while our model is undeniably a simplified realization of any outbreak, the model provides evidence for the considerable efficacy of a 'send unvaccinated students home' policy during outbreaks of measles in communities that are 'close to' versus 'well above' the herd immunity vaccination coverage threshold.

Interestingly, our policy of sending home students during possible outbreaks had a significant impact on the number of cases resulting in communities with both relatively high (95%) and relatively low (85%) vaccination rates. The mean total number of cases (obtained by adding columns in Table 1) without implementing a 'send unvaccinated students home' policy was 395, yet when 4 out of 5 unvaccinated children are sent home in the low vaccinated community alone (i.e., the policy was not applied to the high vaccinated community), the total mean number of cases dropped below 5. The mean duration of these outbreaks (data not shown in Table 1) was also significantly different between the two cases: for the 'no action' case it was 251 days compared with 93 days when the 'send unvaccinated students home' policy was implemented in the low vaccination community alone.

The data, supported by our model, strongly suggest that the 2014–15 measles outbreak in California occurred as a result of the variable vaccination coverage across different communities and the mixing of these communities at superspreading centers. While herd immunity levels may be met at origin locations of visitors to major superspreading centers, such as Disneyland, the ephemeral populations that form each day may have cumulative vaccination rates below the average for California as a whole. Over time, with high enough turnover rates and population sizes, rare disease recurrences are bound to be introduced when superspreading assemblages are below elevated herd immunity thresholds that are associated with high-density tourist aggregation or entertainment centers, which then act as superspreading centers. Conventional wisdom in epidemiology pushes vaccination as the solution to herd immunity, but emerging evidence shows that anti-MMR vaccine populations only become less likely to vaccinate after intervention campaigns.[13] Rather than attempting to reform the attitudes of the substantial minority of people who oppose vaccination for reasons varying from religious objection to distrust of the medical or political establishment, we offer an easily implemented, and politically neutral, mitigation technique. By sending students without proof of vaccination home from school at a success rate of around 80% (interventions are rarely 100% successful) when an outbreak is imminent or present, the number of resulting cases dramatically declines. This policy is effective in communities with relatively high vaccination rates (95%), as well as communities near the herd immunity threshold (85%).

While the 2014 measles epidemic has been effectively suppressed, its reappearance in the US after apparent eradication suggests that future outbreaks should not be unexpected, nor should we be unprepared if one occurs. In addition, the methods applied here can be easily adapted to epidemics of other pathogens, particularly those that are highly transmissible, like influenza virus or coronavirus. In these cases, superspreading centers are likely to play a similarly important role in the spread of the outbreak. Gaining insight into the mechanisms underlying this process is vital, and the conceptual model outlined above offers an opportunity to do so, in addition to simulating

the impact of various 'send unvaccinated students home' policies. Our empirical model of the regional processes also provides a relative risk surface for future disease outbreaks that may be especially useful in the case of another epidemic emerging from a superspreading center.

Acknowledgements

We thank Sarah Ackley for useful discussions on the Californian vaccination rate data.

Funding

TCP was supported by a Models of Infectious Disease Agent Study (MIDAS) grant from the US NIH/NIGMS to the University of California, San Francisco, USA (U01GM087728). WMG was supported by funds from the University of California, Berkeley, USA.

References

1. Chen RT, Goldbaum GM, Wassilak SGF, et al. An explosive point-source measles outbreak in a highly vaccinated population: modes of transmission and risk factors for disease. *Am J Epidemiol* 1989; 129: 173–182.
2. Fine PE and Clarkson JA. Measles in England and Wales? i: an analysis of factors underlying seasonal patterns. *Int J Epidemiol* 1982; 11: 5–14.
3. Bjørnstad ON, Finkenstadt BF and Grenfell BT. Dynamics of measles epidemics: estimating scaling of transmission rates using a time series SIR model. *Ecol Monogr* 2002; 72: 169–184.
4. Keeling MJ and Grenfell B. Disease extinction and community size: modeling the persistence of measles. *Science* 1997; 275: 65–67.
5. Schlenker TL, Bain C, Baughman AL, et al. Measles herd immunity: the association of attack rates with immunization rates in preschool children. *JAMA* 1992; 267: 823–826.
6. Anderson RM and May RM. Vaccination and herd immunity to infectious diseases. *Nature* 1985; 318: 323–329.
7. Shim E, Grefenstette JJ, Albert SM, et al. A game dynamic model for vaccine skeptics and vaccine believers: measles as an example. *J Theor Biol* 2012; 295: 194–203.
8. Albrecht P, Ennis FA, Saltzman EJ, et al. Persistence of maternal antibody in infants beyond 12 months: mechanism of measles vaccine failure. *J Pediatr* 1977; 91: 715–718.
9. Paunio M, Hedman K, Davidkin I, et al. Secondary measles vaccine failures identified by measurement of IgG avidity: high occurrence among teenagers vaccinated at a young age. *Epidemiol Infect* 2000; 124: 263–271.
10. Mossong J and Muller C. Estimation of the basic reproduction number of measles during an outbreak in a partially vaccinated population. *Epidemiol Infect* 2000; 124: 273–278.
11. Rao TS and Andrade C. The MMR vaccine and autism: Sensation, refutation, retraction, and fraud. *Indian J Psychiatry* 2011; 53: 95.
12. Lieu TA, Ray GT, Klein NP, et al. Geographic clusters in under-immunization and vaccine refusal. *Pediatrics* 2015; 135: 280–289.
13. Nyhan B, Reifler J, Richey S, et al. Effective messages in vaccine promotion: a randomized trial. *Pediatrics* 2014; 133: e835–e842.
14. Adams D, Gallagher K, Jajosky R, et al. Summary of notifiable diseases-united states, 2011. *Morb Mortal Wkly Rep* 2013; 60: 1–117.
15. McCarthy M. Measles cases exceed 100 in us outbreak. *BMJ* 2015; 350: h622.
16. Blumberg S, Worden L, Enanoria W, et al. Assessing measles transmission in the united states following a large outbreak in California. *PLoS Currents: Outbreaks* 2015; 7: 7.
17. Paull SH, Song S, McClure KM, et al. From superspreaders to disease hotspots: linking transmission across hosts and space. *Front Ecol Environ* 2011; 10: 75–82.
18. Matthews L, McKendrick I, Ternen H, et al. Super-shedding cattle and the transmission dynamics of *Escherichia coli* o157. *Epidemiol Infect* 2006; 134: 131–142.
19. Lloyd-Smith JO, Schreiber SJ, Kopp PE, et al. Superspreading and the effect of individual variation on disease emergence. *Nature* 2005; 438: 355–359.
20. James A, Pitchford JW and Plank MJ. An event-based model of superspreading in epidemics. *Proc R Soc Lond B Biol Sci* 2007; 274 (1610): 741–747.
21. Chowell G, Hengartner NW, Castillo-Chavez C, et al. The basic reproductive number of Ebola and the effects of public health measures: the cases of Congo and Uganda. *J Theor Biol* 2004; 229: 119–126.
22. Althaus CL. Estimating the reproduction number of Ebola virus (Ebov) during the 2014 outbreak in West Africa. *PLoS currents* 2014; 6.
23. Greenland S. Principles of multilevel modelling. *Int J Epidemiol* 2000; 29: 158–167.
24. Barbour AD and Utev S. Approximating the reed–frost epidemic process. *Stoch Proc Appl* 2004; 113: 173–197.
25. Lloyd-Smith JO, Galvani AP and Getz WM. Curtailing transmission of severe acute respiratory syndrome within a community and its hospital. *Proc R Soc Lond B Biol Sci* 2003; 270: 1979–1989.
26. Getz WM, Gonzalez J-P, Salter R, et al. Tactics and strategies for managing Ebola outbreaks and the salience of immunization. *Comput Math Methods Med* 2015; 1–9.
27. Blumberg S, Enanoria WTA, Lloyd-Smith JO, et al. Identifying post-elimination trends for the introduction and transmissibility of measles in the united states. *Am J Epidemiol* 2014; 179: 1375–1382.
28. Bradford WD and Mandich A. Some state vaccination laws contribute to greater exemption rates and disease outbreaks in the united states. *Health Affairs* 2015; 34: 1383–1390.
29. Lekone PE and Finkenstadt BF. Statistical inference in a stochastic epidemic SEIR model with control intervention: Ebola as a case study. *Biometrics* 2006; 62: 1170–1177.
30. Hethcote HW. The mathematics of infectious diseases. *SIAM review* 2000; 42: 599–653.
31. Getz WM and Lloyd-Smith JO. Basic methods for modeling the invasion and spread of contagious diseases. *DIMACS Ser Discrete Math Theoret Comput Sci* 2006; 71: 87–112.
32. Ferrari MJ, Grais RF, Bharti N, et al. The dynamics of measles in sub-Saharan Africa. *Nature* 2008; 451: 679–684.

33. Bolker B and Grenfell B. Chaos and biological complexity in measles dynamics. *Proc R Soc Lond B Biol Sci* 1993; 251: 75–81.
34. Cauchemez S and Ferguson NM. Likelihood-based estimation of continuous-time epidemic models from time-series data: application to measles transmission in london. *J R Soc Interface* 2008; 5: 885–897.
35. Lloyd AL. Destabilization of epidemic models with the inclusion of realistic distributions of infectious periods. *Proc R Soc Lond B Biol Sci* 2001; 268: 985–993.
36. Getz WM and Pickering J. Epidemic models: thresholds and population regulation. *Amer Nat* 1983; 121(6): 892–898.
37. McCallum H, Barlow N and Hone J. How should pathogen transmission be modelled? *Trends Ecol Evol* 2001; 16: 295–300.
38. Porco TC, Lloyd-Smith JO, Gross KL, et al. The effect of treatment on pathogen virulence. *J Theor Biol* 2005; 233: 91–102.
39. Salter RM. Nova: A modern platform for system dynamics, spatial, and agent-based modeling. *Procedia Comput Sci* 2013; 18; 1784–1793.
40. Getz W, Salter R and Sippl-Swezey N. Using Nova to construct agent-based models for epidemiological teaching and research. In: Yilmaz L, Chan W, Moon I, et al. (eds) *Proceedings of the 2015 Winter Simulation Conference*, 6 December 2015, pp. 3490–3501. Piscataway, NJ: IEEE.

Author biographies

Wayne Getz is a Starker Leopold Professor of Wildlife Ecology at the University of California, Berkeley and an Extraordinary Professor in the Mathematical Sciences at the University of KwaZulu-Natal. He received a PhD degree in Applied Mathematics from the University of the Witwatersrand, South Africa, in 1976, and a DSc in Zoology from the University of Cape Town, South Africa, in 1995. He is a Founding Partner of Numerus, Inc., which releases and maintains NOVA software. Beyond his many research publications, he has coauthored a monograph on Population Harvesting and a textbook on Calculus for the Life Sciences.

Colin Carlson is a fifth-year Ph.D in the Environmental Science, Policy and Management program at UC Berkeley. Colin received a B.S. in Ecology and Evolutionary Biology and a B.A. in Environmental studies at the University of Connecticut Storrs, in 2012, and his M.S. in Ecology and Evolutionary Biology in 2013.

Eric Dougherty is currently a fifth-year PhD student in the Environmental Science, Policy and Management program at UC Berkeley. Eric received a BS in Environmental studies at Washington University in St. Louis, USA, in 2012. His research experience includes field work in South Africa and Australia. He has four scientific publications to date.

Travis Porco Travis Porco is Professor of Epidemiology and Biostatistics at the University of California, San Francisco. His work has concerned mathematical modeling of trachoma, leprosy, tuberculosis, measles, and HIV. He has also served as an NIH clinical trial biostatistician. He received his PhD in Biophysics from UC Berkeley, USA in 1994.

Richard Salter is Professor of Computer Science at Oberlin College. He received his PhD in Mathematics from Indiana University, USA in 1978. He is the author of more than 30 research and educational publications, and the designer of many software applications for industry and education. He is a Founding Partner of Numerus, Inc., which releases and maintains NOVA software. His research has been supported by NSF and ONR.